

Materials Design by Quantum-Chemical and other Theoretical/Computational Means: Applications to Energy Storage and Photoemissive Materials

Károly Németh^{*a}

DOI: 10.1039/b000000x

The present paper discusses some recent developments in the field of rational design for energy storage and photoemissive materials. Recent and new examples of designer materials for Li-ion and Li-air type batteries with high capacity and energy/power density as well as photoemissive materials with low workfunctions and improved brightness are discussed as illustrative examples of how quantum-chemical and other theoretical computational means can be used for rational materials design.

1 Introduction

Rational materials design has been one of the holy grails of chemistry and physics. With the advent of efficient algorithms that solve the Schrödinger equation at various levels of approximation in (near) linear scaling computational effort¹ as compared to the system size, combined with parallel computers using ever faster processors, this goal is now within reach and the fruits of decades of hard work in the development of such methodologies are increasingly harvested in terms of rationally designed materials. Major projects funded by governments or by the industry invest substantial funds in rational materials design. The US government funds the Materials Genome Initiative to computationally explore, design and experimentally test designer materials with approximately 100 million dollars through various agencies, such as NSF and DOE. Major materials design efforts are also underway in other programs as well, for example within the Joint Center of Energy Storage Research (“Battery Hub”) program of DOE as electrode materials and electrolyte design efforts. Similar initiatives can be seen in the private industry as well. For example, Bosch, a major supplier of electrical appliances conducts systematic computational materials screening and design efforts in the fields of energy storage and conversion. Major companies, such as IBM, Bosch, and Apple produce thousands of patent applications each year. More than half a million patent applications are filed in the US annually, and about a quarter of a million patents are granted. There is an increasing number of patents solely based on theoretical materials design (“conceptual reduction to practice”) without experimental testing (“actual reduction to practice”) that can also be attributed to the increased competition in the race for materials that can potentially control important emerging fields of applications, such as energy storage, clean energy production, etc.²⁻⁴. Patents have always been formulated so that they cover an as broad as possible range of potential modifications

of the core invention, leading sometimes to extremely broad patents, such as Intel’s one on all nanostructures smaller than 50 nm in diameter or Rice University’s one on all objects composed at least 99% of carbon nanotubes⁵.

The vast majority of the materials design efforts for the exploration of crystalline materials use electronic structure codes with periodic boundary conditions such as VASP⁶ or Quantum Espresso⁷. These codes utilize plane wave representation of wavefunctions, effective pseudopotentials to model core electrons and various exchange and correlation functionals within the DFT approach. While these codes and the underlying methods have severe limitations for certain phenomena, such as electron correlation effects, band gaps in transition metal compounds, intermolecular interactions⁸, excited state properties, etc., effective core potentials, exchange/correlation potentials and novel DFT correction methodologies have been developed to cure some of these problems. These latter methods include the DFT+U⁹ method that turned out particularly practical for studying band gaps, thermo/electro-chemistry, phase changes, magnetic states and structural properties of solids. Gaussian and mixed Gaussian-plane-wave representation based codes, as well as wavelet or adaptive grid based ones are also used in the exploration of materials. Such codes include SIESTA¹⁰, Gaussian¹¹, PQS¹², FreeON¹³, to name a few. Some of these codes are also capable to calculate explicit electron-electron correlation with periodic boundary conditions, for example utilizing quasiparticle (electron-pair) bands on the MP2 level of correlation and beyond¹⁴.

Other approaches to materials design may be based on the “mining” and analysis of existing data deposited in the scientific literature, with the aim of revealing potentially useful but yet unobserved or unutilized connections and thereby constructing new structures/compositions of materials that are potentially superior to existing and well observed ones¹⁵.

The present perspectives paper will focus on some recent

developments in the field of materials design for Li-ion and Li-air batteries first, then describes approaches about the development of improved photoemissive materials.

2 Results and Discussion

2.1 Li-ion batteries

Most Li-ion batteries operate through the intercalation and deintercalation of Li-ions in the positive electrode (cathode of the discharge process) electroactive materials. There is a great effort to optimize the properties of the electroactive crystals. The optimization parameters include the gravimetric and volumetric energy densities of the electroactive materials, their capacities (concentration of Li that can intercalate), the power densities (how fast the charging and discharging may occur), the voltage associated with the corresponding electrochemical reaction, the electrolytes that have to sustain the voltages and currents that occur and the economy of the materials involved, to name a few optimization parameters. Most design efforts focus on layered crystalline cathode materials, such as spinels or polyanionic compounds^{16,17}. In order to computationally predict the voltage associated with an electrochemical cell reaction, one has to calculate the Gibbs free energy change associated with the reaction, express it in terms of eV-s and divide by the number of electrons transferred during the reaction per molecule of product. The reaction energy is almost always approximated as the difference of the electronic energies of the products and reactants which is usually a good approximation when no gas molecules are involved that would cause large entropy changes¹⁷⁻¹⁹. However, the accurate calculation of reaction energies and other properties of solids is often problematic, especially in case of transition metal compounds. It turns out, that DFT(GGA)+U methods are capable to provide reaction energies and voltages that compare well with experiments for this class of materials¹⁷⁻¹⁹. Perhaps the best intercalation material designed for cathode applications so far, is $\text{Li}_3\text{Cr}(\text{BO}_3)(\text{PO}_4)$ a polyanionic material with sidorenkite ($\text{Na}_3\text{MnPO}_4\text{CO}_3$) structure¹⁷. This material has not been synthesized yet. Lithium intercalation in the deintercalated $\text{Cr}(\text{BO}_3)(\text{PO}_4)$ structure occurs at calculated voltages of 4.2-5.1 V, relative to Li/Li^+ , resulting in theoretical energy densities of 1705 Wh/kg and 4814 Wh/L with capacities of 354 mAh/g¹⁷. For comparison, LiCoO_2 cathode materials in current Li-ion batteries have a theoretical energy density of 568 Wh/kg (2868 Wh/L) and charge capacity of 273 mAh/g (1379 mAh/cm⁻³)⁴.

While the energy density of $\text{Li}_3\text{Cr}(\text{BO}_3)(\text{PO}_4)$ and related materials is very attractive, their power density (the rate of charging and discharging) remains low, as the process of intercalation/deintercalation is relatively slow, rendering the charging of Li-ion batteries typically an overnight long process. To

develop materials with both high power and energy densities, the present author has recently proposed²⁰ the use of functionalized hexagonal boron nitride (h-BN) monolayers as intercalation materials. In this case the intercalation would happen into the surface of a 2D material directly from the electrolyte, avoiding the slow diffusion inside the crystallites. The charging process would be similarly fast, allowing for large current densities. Here, two materials based on BN are briefly discussed. The first one is a 3D material, Li_3BN_2 , the second one is a 2D one, BNCN, a cyano (-CN) group functionalized h-BN.

2.1.1 Li_3BN_2 It has been known for decades that the reaction of molten Li_3N with h-BN can produce various phases of the Li_3BN_2 crystalline material²¹. $\alpha\text{-Li}_3\text{BN}_2$ has a layered structure as shown in Fig. 1, with two Li ions being mobile per formula unit, while the third Li is part of a 1D rod-like polymer, with repeating -Li-N-B-N- sequence. The polymeric chains and the mobile Li ions are placed in separate layers in the $\alpha\text{-Li}_3\text{BN}_2$ phase (space group $\text{P4}_2/\text{mnm}$). The cell reaction proposed²⁰ is $2\text{Li} + \text{LiBN}_2 \rightarrow \text{Li}_3\text{BN}_2$ on discharge. The formal charge of the BN_2^{n-} linear anion changes from $n=-1$ to $n=-3$ on discharge. Since no heavy transition metal atoms are involved, one may use the PBEsol functional^{22,23} to obtain realistic optimum crystal structures and reaction energies. The Quantum Espresso⁷ software has been used, with ultrasoft pseudopotentials and 50 rydberg wavefunction cutoff, using a 6x6x6 k-space grid. The residual forces were smaller than 1.d-4 Ry/bohr at the optimum structures. Experimental lattice parameters $a=b$ and c have been reproduced with an accuracy of smaller than 1% and 2.5% errors, respectively. Note that the c -direction is perpendicular to the layers mentioned. In the Li-deintercalated structure, the lattice parameters $a=b$ and c become 1.2 and 3.3 % shorter, which indicates a cell volume shrinking of 5.6 %, or 2.8% per two-electron transfer. Note that such a relatively small cell volume change counts as acceptable for Li-ion battery electrode applications¹⁷. The cell reaction energy is calculated to be $\Delta E = -7.23$ eV, indicating a cell voltage of $U=3.61$ V (assuming an Li/Li^+ anode). The gravimetric and volumetric energy densities are 3247 Wh/kg and 5919 Wh/L, respectively. These values are significantly larger than those obtained for $\text{Li}_3\text{Cr}(\text{BO}_3)(\text{PO}_4)$ ¹⁷. Especially the gravimetric energy density is almost twice as large for Li_3BN_2 as for $\text{Li}_3\text{Cr}(\text{BO}_3)(\text{PO}_4)$. Li_3BN_2 appears to be greatly superior to $\text{Li}_3\text{Cr}(\text{BO}_3)(\text{PO}_4)$ also in terms of gravimetric and volumetric capacity densities with the respective values of 899 mAh/g and 1638 mAh/cm³. It is surprising that Li_3BN_2 has not been tested as cathode electroactive material yet. The reason is probably that only the alpha phase can be expected to preserve its layered structure after the deintercalation of mobile Li-ions. The monoclinic phase has been considered recently for application as part of a con-

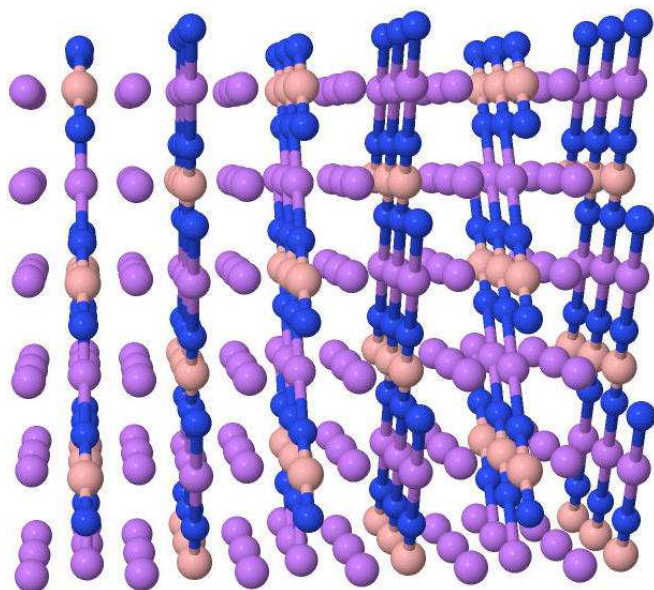


Fig. 1 Perspective view of the layered structure of α - Li_3BN_2 in a $3 \times 3 \times 3$ supercell. Color code: Li - violet, B - magenta, N - blue.

version based anode material²⁴. The high melting point of α - Li_3BN_2 , about 900°C ²¹ is also indicative of the stability of the polymeric chains with $-\text{Li-N-B-N-}$ repeating units, as the Li ions that are not incorporated in the chains are known to be very mobile as excellent Li-ion conductivity values indicate²¹. Therefore, the present calculations also predict the existence of stable phases with the stoichiometry of Li_xBN_2 with $1 < x < 3$. Furthermore, potentially also the beta and the monoclinic phase would be transformed to α - Li_3BN_2 after repeated charge/discharge cycles, as the alpha phase appears as the energetically most favorable packing of the polymeric $-\text{Li-N-B-N-}$ rods.

2.1.2 BNCNNa The reaction of molten sodium cyanide with h-BN is expected to lead to the cyano-functionalization of B sites on both sides of the h-BN monolayers which then intercalate Na^+ ions, as depicted in Fig. 2. This structure is expected to lead to fast charging and discharging due to the sterically unhindered access of Na^+ ions to the intercalation sites. Using the above methodology and a $\approx 30 \text{ \AA}$ vacuum layer to separate layers of BNCNNa, the electrochemical properties of BNCNNa have been computed. Both intercalated and deintercalated structures are stable and preserve the covalent cyano functionalized B centers. With Li atoms instead of Na, the covalent functionalization would break up and LiCN and h-BN would form. The voltage of the $\text{Na} + \text{BNCN} \rightarrow \text{BNCNNa}$ electrochemical cell is calculated to be $U = 2.87 \text{ V}$, associated with a cell reaction energy of 2.87 eV (assuming an Na/Na^+ anode). The gravimetric and volumetric energy densities are 1042 Wh/kg and 3547 Wh/L , the capacity

values 363 mAh/g and 1236 mAh/cm^3 . These values indicate great potential for example for use in portable electronics devices. BNCN and analogous functionalized h-BN compounds can serve as universal intercalation electrode materials capable to intercalate alkali, alkaline earth, Al and other cations (unless conversion reactions happen) thus allowing for batteries based on the transfer of cations other than Li^+ .

Note that in principle similar functionalization of graphene can also be envisioned, however the patterned and polarized h-BN surface is a much better candidate for electrophile and nucleophile attack by functionalization agents, such as molten salts. In case of graphene, all atoms are equivalent for functionalization, while for h-BN only half of the atoms can be subject of, say, nucleophile attack, leaving the other half unfunctionalized providing space for intercalation of cations and free N atoms in the BN surface to contribute to the complexation and binding of the intercalating ions as well as to the storage of the extra negative charge per formula unit due to discharge. Therefore, h-BN appears to be a better candidate to build 2D intercalation structures than graphene. Doped graphene structures may have similar properties to h-BN for covalent functionalization. Functional groups should be selected based on whether they make h-BN a strong electron acceptor after the functionalization, when positive electrode materials are designed. For negative electrode materials, the functional group should be selected such that the resulting layer will be a good electron donor. These considerations are analogous to the design of charge transfer salts²⁵.

While transition metal compounds currently dominate Li-ion battery electroactive materials, there is a lot of potential in conjugated π -electron systems and their functionalized derivatives to be utilized as electroactive materials. Concepts of these systems, such as the principles of charge transfer compounds, have practically been completely ignored in energy storage development so far. As a direct continuation of the present work, a great variety of functionalization of h-BN will be explored to find the best novel anode and cathode materials of this class of compounds. Band structures, conductivities, charge distributions and structural changes upon intercalation/deintercalation will be analyzed to understand the mechanism of charge storage in these materials. The experimental testing of some of these materials is already underway through collaborative work at Illinois Institute of Technology and elsewhere.

2.2 Li-air batteries

Li-air batteries are considered as the ultimate large energy density batteries that would enable long range all electric vehicles. They produce electrical energy through the reaction of metallic Li with O_2 taken from the air, whereby the discharge product must be Li_2O_2 in order the battery be recharge-

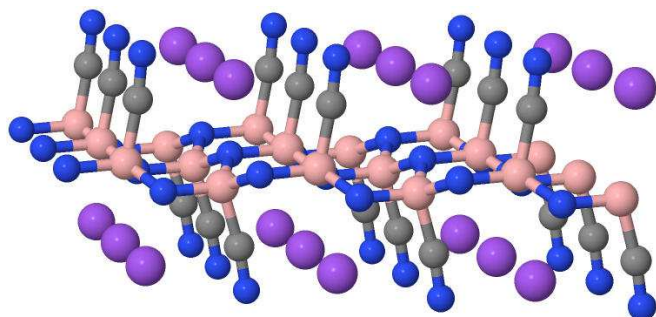


Fig. 2 Perspective view of the cyano functionalized h-BN monolayer with intercalated Na ions in a $3 \times 3 \times 1$ supercell. Color code: Na - violet, B - magenta, N - blue, C - gray.

able. The fact that Li_2O_2 is an aggressive oxidant and may explosively oxidize the carbon electrode in which it forms and deposits makes Li-O₂/peroxide batteries unsafe. A thorough analysis¹⁵ by the present author about the thermochemistry and kinetics of Li-oxalate, $\text{Li}_2\text{C}_2\text{O}_4$, with the availability of catalysts for selective and energy-efficient CO_2 /oxalate conversions indicates that instead of O_2 , CO_2 should be taken from air (or from a tank) to construct a high energy and power density battery that can be safely used and is of environmentally benign and economic materials. The details of the design based on existing experimental data can be found in Ref. 15. A key component of the energy-efficiency of CO_2 /oxalate cathodes is the catalyst that reduces the overpotential of CO_2 reduction to nearly zero. While such catalysts are known, for example copper complexes or oxygen molecule in selected ionic liquid electrolytes¹⁵, the applicability of these catalysts may vary in the various implementations, therefore there is a need for the development of additional robust catalysts to optimize the performance of metal- CO_2 /oxalate batteries.

2.3 Photoemissive materials

Another example of materials design discussed here concerns photoemissive materials. Improved photocathodes are needed for future electron and light sources, such as x-ray free electron lasers, energy recovery linacs and dynamic and ultrafast transmission electron microscopes. The improvements must concern the brightness, the quantum yield, the workfunction and the chemical inertness and lifetime of the photocathodes. Some of our recent works provide examples of related designs^{26–28}. In the first example, we have shown²⁶ using band structure calculations that the angular distribution of emitted electrons can drastically change when depositing an ultrathin (2–4 monolayers) MgO layer on the Ag(001) crystal surface. While a lot of electronic structure studies have been carried out on the MgO:Ag(001) system to explain the experimentally observed variation of its catalytic activity with varying

number of MgO monolayers, we were the first to propose using this variation to optimize the brightness (angular distribution) of emitted electrons through overlayer deposition. Recent experimental results²⁹ have confirmed our predictions and point out the drastic change in the angular distribution of emitted electrons due to MgO overlayers on Ag(001). Ultrathin oxide monolayers over metal surfaces change the electrostatic boundary conditions on the surface and thus they may significantly decrease or increase the workfunctions and the shape and occupation of surface bands which leads to drastic changes in the properties of the emitted electrons²⁶. In the second example, we have pointed out that the workfunction of the seasoned, high quantum efficiency Cs_2Te photoemissive material can be lowered from ≈ 3 eV to about 2.4 eV by acetylation resulting in Cs_2TeC_2 while its quantum efficiency is preserved²⁷. Analogous compounds Cs_2PdC_2 and Cs_2PtC_2 exist and we have managed to synthesize Li_2TeC_2 (x-ray diffraction confirms theoretically predicted structure)³⁰ as the first member of ternary acetylides with Te. This design was motivated by the goal of turning Cs_2Te into an easier to excite π -electron system. Our current research directions in the photocathode field focus on the theoretical screening of various inorganic and organic overlayers on metals and semiconductors to lower workfunctions, optimize brightness, quantum yield and life time of such photocathodes in the often harsh temperature, imperfect vacuum and electromagnetic field environments they are used.

3 Conclusions

The present paper discusses several examples of materials design using quantum chemical and other theoretical / computational methods to develop improved Li-ion and Li-air batteries and improved photoemissive materials. The experimental testing of some of these designs is underway.

4 Acknowledgements

Discussions with Drs. L. Shaw (IIT), K. C. Harkay and G. Srajer (Argonne) are gratefully acknowledged. The Li-air battery and the photocathode research has been supported by the U.S. DOE Office of Science, under contract No. DE-AC02-06CH11357 and NSF (No. PHY-0969989).

References

- 1 *Linear-Scaling Techniques in Computational Chemistry and Physics*, ed. R. Zalesny, M. G. Papadopoulos, P. G. Mezey and J. Leszczynski, Springer, Berlin, Heidelberg, New York, 1st edn, 2011, vol. 13.

^a Address: Physics Department, Illinois Institute of Technology, Chicago, Illinois 60616, USA, nemeth@agni.phys.iit.edu

- 2 P. Albertus et al., *High Specific Energy Li/O₂-CO₂ Battery; assignee: Bosch LLC; US Patent Application 12/907,205*, 2010.
- 3 S. C. Jones et al., *Polymer Materials As Binder for a CFx Cathode; assignee: Contour Energy Systems Inc.; US Patent Application 13/010,431*, 2011.
- 4 K. Nemeth, M. van Veenendaal and G. Srajer, *Electrochemical energy storage device based on carbon dioxide as electroactive species, assignee: US. Dept. of Energy, Patent (granted), US8389178*, 2013.
- 5 J. M. Pearce, *Nature*, 2012, **491**, 519–521.
- 6 J. Hafner, *J Comput Chem* 29: 20442078, 2008, 2008, **29**, 20442078.
- 7 P. Gianozzi et al., *J. Phys.: Condens. Matter*, 2009, **21**, 395502.
- 8 J. Paier et al., *J. Chem. Phys.*, 2006, **124**, 154709.
- 9 V. I. Anisimov et al., *Phys. Rev. B*, 1991, **44**, 943.
- 10 Soler, Jos M. et al., *J. Phys. Cond. Mat.*, 2002, **14**, 2745.
- 11 M. J. Frisch et al., GAUSSIAN09, 2013, Gaussian, Inc., Wallingford CT, <http://www.gaussian.com>.
- 12 J. Baker et al., *WIREs Comput. Mol. Sci.*, 2012, **2**, 63.
- 13 N. Bock, M. Challacombe, C. K. Gan, G. Henkelman, K. Nemeth, A. M. N. Niklasson, A. Odell, E. Schwegler, C. J. Tymczak and V. Weber, FREEON, 2013, Los Alamos National Laboratory (LA-CC 01-2; LA-CC-04-086), Copyright University of California., <http://www.freeon.org/>.
- 14 S. Suhai, *Phys. Rev. B*, 1983, **27**, 3506.
- 15 K. Németh and G. Srajer, *RSC Advances*, 2014, **4**, 1879.
- 16 B. C. Melot and J.-M. Tarascon, *Acc. Chem. Res.*, 2013, **46**, 1226–1238.
- 17 G. Hautier et al., *J. Mater. Chem.*, 2011, **21**, 1714717153.
- 18 F. Zhou et al., *Electrochem. Comm.*, 2004, **6**, 1144–1148.
- 19 A. Jain et al., *Phys. Rev. B*, 2011, **84**, 045115.
- 20 K. Nemeth, *Functionalized Boron Nitride Materials as Electroactive Species in Electrochemical Energy Storage Devices, patent pending, assignee: Nemeth's Materials Design LLC*, 2013.
- 21 H. Yamane et al., *J. Solid State Chem.*, 1987, **71**, 1–11.
- 22 J. P. Perdew, K. Burke and M. Ernzerhof, *Phys. Rev. Lett.*, 1996, **77**, 3865.
- 23 J. P. Perdew et al., *Phys. Rev. Lett.*, 2008, **100**, 136406.
- 24 T. H. Mason et al., *J. Phys. Chem. C*, 2011, **115**, 16681–16688.
- 25 J. Huang et al., *Phys. Chem. Chem. Phys.*, 2008, **10**, 2625.
- 26 K. Németh, K.C. Harkay et al., *Phys. Rev. Lett.*, 2010, **104**, 046801.
- 27 J. Z. Terdik and K. Németh et al., *Phys. Rev. B*, 2012, **86**, 035142.
- 28 A. Ruth and K. Németh et al., *J. Appl. Phys.*, 2013, **113**, 183703.
- 29 T. C. Droubay et al., *Phys. Rev. Lett.*, *submitted*, 2013.
- 30 K. Németh, A. K. Unni and J. Kaduk et al., *The synthesis of ternary acetylides with Te, to be published*.